

Long-Wavelength Waveguide Photodiodes for Optical Subscriber Networks

by Masaki Funabashi*, Koji Hiraiwa*, Kazuaki Nishikata*²,
Nobumitsu Yamanaka*, Norihiro Iwai* and Akihiko Kasukawa*

ABSTRACT Waveguide photodiodes hold promise for long-wavelength applications in optical subscriber networks, and this paper reports on the methods used in their design and manufacture, as well as on the results obtained from prototype devices. With a view to the improved productivity and reduced cost associated with volume manufacture, the prototype were fabricated by a full-wafer process using 2-inch InP wafers. The device showed an extremely low dark current value --only a few hundred pA --and high responsivity --0.95 A/W or above. Characteristic deviation within wafers was evaluated, confirming that 2-inch wafers having high in-wafer uniformity with respect to dark current and responsivity could be produced with high yield. The devices had a frequency bandwidth of approximately 4 GHz and a vertical coupling tolerance of 4 μ m, with low intermodulation distortion and high reliability.

1. INTRODUCTION

Keen expansion of the Internet and an increase in demand for large capacity transmission have forced us to use optical fibers in the telecommunication networks. Furukawa Electric supplies various devices needed for such optical telecommunication systems. We have developed and are producing: optical fibers which are a major breakthrough in optical telecommunication; semiconductor lasers used as a light source; optical amplifiers necessary for long distance telecommunication; photodiodes which receive optical signals and convert them into electric signals and so on. These devices are essential to the optical telecommunication systems. This paper reports on the development of a photodiode which converts optical signals into electric signals.

Photodiodes used for optical telecommunications are divided into two categories by their shapes, one is a surface-illuminated type, the other is a side-illuminated (waveguide) type. Furukawa's R&D center has been developing the latter devices, Waveguide Photodiodes (WGPD) which were considered to be widely acceptable in future. Figure 1 shows a view of the photodiode, and Figure 2 shows a cross-sectional structure of the same.

As shown in Figure 1, the WGPD has a shape similar to an ordinary edge-emitting laser, and receives light signals at the edge surface of the device. The incident light travels along the waveguide and attenuates gradually by absorption. Photocarriers, which are generated as light is ab-

sorbed, are pulled out by a reverse-biased voltage and converted into electrical current signals.

As shown in the figures, the incident direction of light and the current flowing direction differ from each other. Therefore, the length and thickness of the absorber can be independently decided both from the electrical view point or the optical view point. This advantageous feature makes it possible to simultaneously design the WGPD in terms of high-speed and high responsivity. Also by adopting a structure which absorbs light uniformly along the waveguide, it is possible to achieve low intermodulation distortion with high responsivity. In an optical access CATV network, images are optically transmitted in analog signals, therefore low intermodulation distortion characteristics or high linearity photodiodes are largely demanded. Thus, design-free WGPDs are suitable for these analog applications. Another feature of the WGPD is that it is suitable for surface-mount technology. Surface-mount technology is one of the most excellent mounting methods

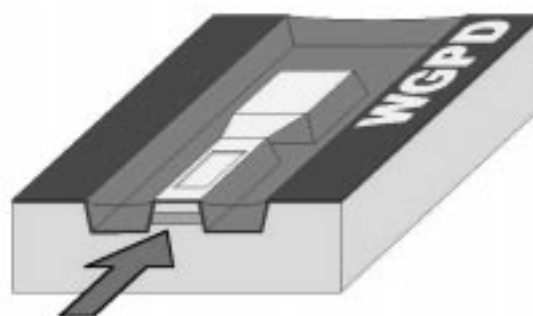


Figure 1 View of WGPD

* Semiconductor R&D Center, Yokohama Lab., R&D Div.
*² Furukawa Electric Technologies, Inc.

that receive widespread attention and provides optically functional devices by integrating several waveguide type optical devices on the platform surface of a Si-wafer. Surface-mount technology is more than appropriate for the production of low cost optical modules.

Recently the quantity of user information is rapidly increasing, therefore subscriber networks are adopting optical fibers, resulting in the need for low cost optical devices. Thus, we have carried out the development of WGPD of low cost and mass-production type over a full-wafer process using 2 inch-wafers to evaluate the in-wafer uniformity of the device characteristics. The result of the study is reported here.

This paper describes a design method of WGPDs in chapter 2 and introduces a design guide based on our method. In chapter 3, device fabrication procedures, mainly with 2-inch full process, are reported. In chapter 4, the characteristics of the device fabricated and in-wafer uniformity in 2-inch process are reported. The last chapter 5 discusses the conclusion.

2. DEVICE DESIGN

The key of the WGPD design is the size of the absorber. This chapter illustrates the optimum design method for the thickness, length and width of the absorber to meet the specification required. In addition, two examples of WGPD design are introduced: the digital design exhibits wide coupling tolerance and high responsivity, while the analog design features low intermodulation distortion and high responsivity, as well.

2.1 Design of Layer Structure

Firstly, the design in thickness direction of a layer structure is described. The layer structure employs a pin-type double-hetero diode structure. It may be said that the electric characteristics of a photodiode (high speed, low intermodulation distortion, etc.) depend on the thickness of the i-layer, and the optical properties (coupling efficiency, etc.) depend on the thickness of the core layer (whose refractive index is larger than that of the cladding layer). As illustrated in Figure 2, i-type absorber is sandwiched by InP cladding layers of p-type and n-type. Optical con-

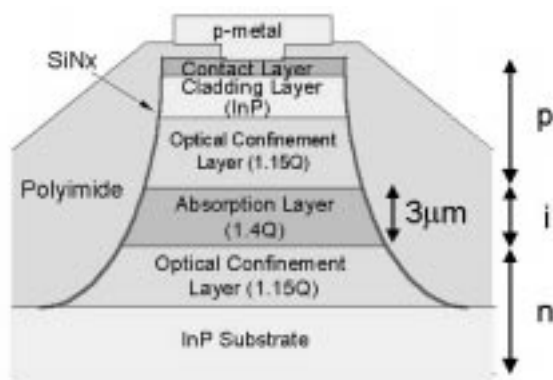


Figure 2 Cross-sectional layer structure of WGPD

finement layers which have an intermediate refractive index are introduced between the absorber and the cladding layers to achieve independent optimizations of both electric characteristics and optical properties. In Figure 2, "1.15Q" means that the layers are a GaInAsP layer of 1.15 μm in bandgap wavelength.

2.1.1 Optimization of Optical Property (Coupling Efficiency)

In this chapter, the design for high coupling efficiency in the WGPD with a single mode optical fiber is described. This coupling efficiency is especially important in the optical properties. In order to acquire high coupling efficiency, it is necessary to design the size of mode field diameter of optical fiber and that of waveguide in the photodiode to be same. Therefore, a multi-mode waveguide structure is adopted¹⁾. The multi-mode waveguide type in WGPDs has an advantage of less degradation in coupling efficiency even when their axis orientations are shifted between the optical fiber and the WGPD, as compared with the single mode waveguide. The simulation results of optical confinement factor into the absorber and mode field diameter of fundamental mode versus the absorber thickness are shown in Figure 3, in the condition when the total layer thickness of the absorber and the optical confinement layers is constant (5 μm). Figure 3 shows that the optical confinement factor is monotonously increasing with the absorber thickness, while the mode field diameter has a tendency of increasing in both thinner and thicker ranges in the absorber thickness. Therefore, in order to obtain the high coupling efficiency, there come two solutions, the absorber thickness must be thickened, or just opposite, must be thinned. However, in consideration of the coupling tolerance in the case of axis mismatching, the thicker absorber layer is better for less degradation in the responsivity because optical confinement factor is large in the higher order modes.

2.1.2 Optimization of Electric Characteristics

The electric characteristics remarkably affected by the layer structure are junction capacitance and intermodulation

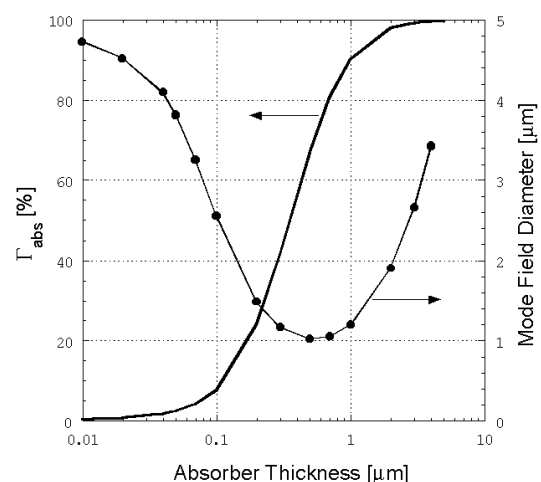


Figure 3 Simulation results of confinement factor and mode field diameter versus absorber thickness

distortion (linearity). The junction capacitance cannot be too large unless i-layer becomes so thinned. In order to acquire low intermodulation distortion in analog type, it is necessary to thin the absorber layer for reducing the quantity of optical absorption per unit length. Thus, it is possible to suppress the space-charge effect caused by the localization of photocarriers.

2.2 Design of Waveguide Length

The waveguide length must be designed to absorb all of the incident light. Shorter waveguide length reduces responsivity, while too longer waveguide degrades the high-speed characteristics. In order to absorb more than 95% of light, the following formula must be adopted:

$$\exp(-\Gamma\alpha L) < 1-0.95$$

where, Γ is the optical confinement factor into the absorber, α is the absorption coefficient, L is the length of the waveguide. For example, $\Gamma=10\%$, $\alpha=10^4 \text{ cm}^{-1}$, then $L > 30 \mu\text{m}$.

2.3 Design of Waveguide Width

The waveguide width is mainly determined by the junction capacitance, coupling tolerance and the ease of the fabrication process. Narrower width can reduce the capacitance, but the coupling tolerance becomes severe and fabrication process becomes difficult.

2.4 Design Examples

Two types of WGPDs, digital and analog, based on the design guideline mentioned above, are introduced. Table 1 exhibits the structure of the two types.

2.4.1 Digital WGPD Design

One design, which has high coupling efficiency with a single mode optical fiber (high responsivity) and has a wide range of coupling tolerance, is introduced here.

This design was intended to use the device at $1.3 \mu\text{m}$ wavelength band, the absorber is made of a GaInAsP layer with $1.4 \mu\text{m}$ band-gap. This absorber is sandwiched by optical confinement layers of GaInAsP with $1.15 \mu\text{m}$ band-gap. The thickness of the absorber is $3 \mu\text{m}$ and those of optical confinement layers are $2 \mu\text{m}$ each, all thickened sufficiently to obtain wider ranges of coupling tolerance. The optical confinement factor into the absorber is as large as about 99 % in fundamental mode, therefore the length

of the waveguide is just enough in several μm s under an optimum coupling condition. In consideration of the coupling tolerance and the easiness of fabrication, the length is decided as $L = 60 \mu\text{m}$, the width of waveguide is also decided as $30 \mu\text{m}$.

2.4.2 Analog WGPD Design

Since low intermodulation distortion characteristics are essential in analog WGPDs, it is necessary to limit the quantity of light absorption per unit length by reducing the thickness of the absorber. This reduction makes it possible to limit the generation of photocarriers in a certain spot and to prevent the space-charge effect, which is the cause of the degradation of linearity. The sample adopted a GaInAs absorber $0.05 \mu\text{m}$ thick, and the thickness of both upper and lower optical confinement layers was $3 \mu\text{m}$ to obtain a high coupling efficiency by enlarging the mode field diameter. Thus in this structure, the optical confinement factor into the absorber is as small as approximately 5% in fundamental mode, and the quantity of light absorption per unit length is also small, the length of the waveguide is determined as $150 \mu\text{m}$, and the width of waveguide is defined as $18 \mu\text{m}$ to reduce junction capacitance.

3. FABRICATION

In this chapter, the results of fabrication of WGPDs on a 2-inch wafer to achieve low cost mass-production are described²⁾. Firstly, a layer structure was grown on the InP wafer, shown in Figure 2, by the use of MOCVD crystal growth equipment. As mentioned above, the layer thickness was very thick as $10 \mu\text{m}$ for high coupling efficiency and wide coupling tolerance. Slight lattice mismatching to the wafer is inevitably generated because of the thick quarterly layers of GaInAsP in the absorber and the optical confinement layers. We tried to control the quantity of the lattice mismatching to be less than 100 seconds in X-ray diffraction measurement, however, because of the thick growth layers, the wafer was warped by the accumulated lattice mismatching even in a slight lattice mismatching rate. Sometimes we experienced in-wafer warp as large as $40 \mu\text{m}$. It is understood that the cause of the warp is due to the stress distortion by the lattice mismatching between the InP wafer and the grown layer. This effect was confirmed by the fact that the direction of warp (dome-shape / bowl-shape) and the direction of the lattice mismatching (compressive / tensile) were consistent.

Because of this wafer warp, sometimes there happened troubles of wafer crack during the photo-lithography process using the conventional contact-type mask aligner. In order to solve the warp problem, we deposited a SiNx film on the back of the wafer to cancel out the warp of wafer. Our experiment showed that the SiNx thin film deposited on the surface of an InP wafer by the plasma-CVD would enhance the warp in bowl-shape in proportion to the film thickness. We tried to control the warp of the wafer using this physical property. The improvement of the flatness was confirmed after the deposition of a 300 nm thick SiNx film

Table 1 Examples of design for digital and analog WGPDs

	Digital	Analog
Contact layer	1.55Q, 0.3 μm thick	1.55Q, 0.3 μm thick
p cladding layer	InP, 2 μm thick	InP, 2 μm thick
Optical confinement layer	1.15Q, 2 μm thick	1.15Q, 3 μm thick
Absorption layer	1.4Q, 3 μm thick	InGaAs, 0.05 μm thick
Optical confinement layer	1.15Q, 2 μm thick	1.15Q, 3 μm thick
n cladding layer	InP, 2 μm thick	InP, 2 μm thick

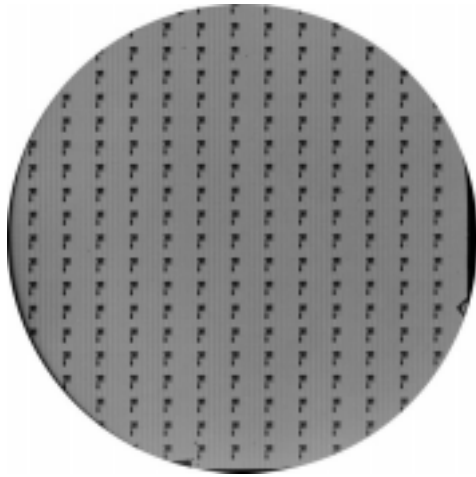


Photo 1 Photograph after 2-inch full wafer fabrication process

on the back of the wafer which had a $36\mu\text{m}$ bowl-shape warp. The amount of warp was reduced down to $4.4\mu\text{m}$ to clear the problem during the photo-lithography process.

The stripe patterns were formed on the flattened wafer by photo-lithography, and wet chemical etching was carried out to the depth through the absorber and the optical confinement layers to form a mesa structure. Because of the etching through quarterly layers, the thick epitaxial layer is divided into many small areas, so the warp of the wafer is much reduced. The size of stripes is $30\mu\text{m}$ wide, $60\mu\text{m}$ long for digital type, and $18\mu\text{m}$ wide, $150\mu\text{m}$ long for analog type.

After forming the mesa-stripe, thin SiN_x insulation film is formed for passivation. Forming the mesa-structure inevitably makes a much uneven surface, therefore, a polyimide film is deposited to flatten the surface. Then a contact window is formed on the mesa-stripe to deposit an upper electrode, and after polishing the wafer to reduce the thickness, finally a lower electrode is deposited.

The wafer surface is shown in Photo 1, which is fabricated by a full-wafer process using a 2-inch InP wafer. The chip-size of the device is $250\mu\text{m}$ wide and $300\mu\text{m}$ long, therefore, the devices of about 20,000 pieces are obtained by excluding the area of 3 mm wide periphery of the wafer.

After the wafer process, arrayed device bars are cut off from the wafer by cleaving, and a SiN_x film for anti-reflection is formed on the incident edge of the device. Lastly, bars are cleaved into chips and arrays of the desired channel number.

4. CHARACTERISTICS

Followings are the characteristics of WGPDs.

4.1 Dark-current and Capacitance

Figure 4 shows an example of dark-current / voltage characteristics. The device shows a very small dark-current of 83 pA at 3 V reverse bias voltage. The result in Figure 4 is derived from the digital type device. As mentioned above,

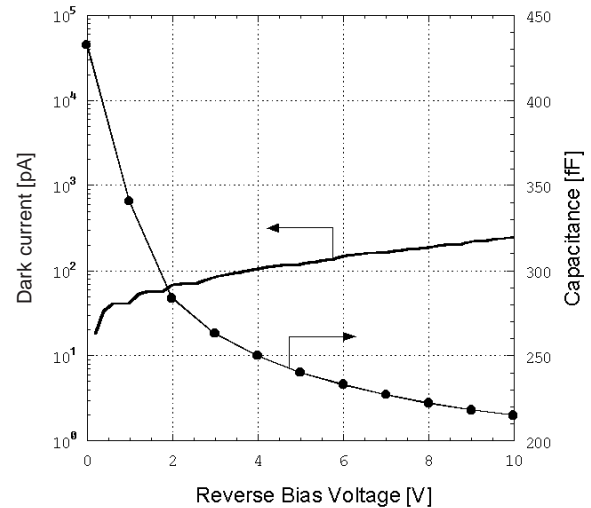


Figure 4 Reverse bias voltage dependence of dark-current and capacitance

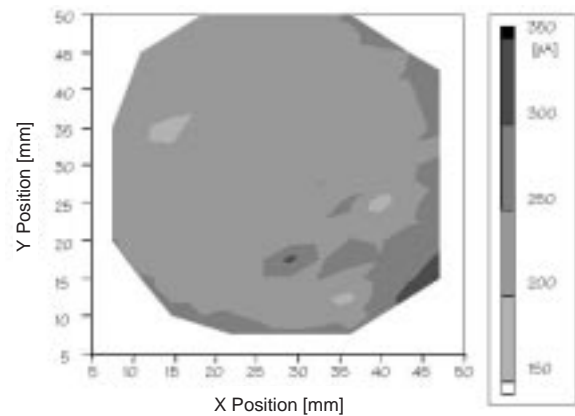


Figure 5 Dark-current distribution in 2-inch wafer

the device in analog type and the device in digital type differ with each other in layer structure, but both dark-currents are low and of the same level.

Figure 4 also shows the voltage dependence of capacitance. Upon applying a reverse bias voltage to the device, the depletion layer spreads to reduce the device capacitance. Very small capacitance of about 215 fF can be obtained at 10 V .

The dark-current distribution of WGPDs on the wafer surface fabricated by 2-inch full process is evaluated through sampling measurements. The result of the dark-current mapping is shown in Figure 5. The measurement was carried out at a bias voltage of 5 V . The result shows that the average dark-current is 238 pA , and standard deviation is 24 pA , indicating the good uniformity of low dark-current distribution except the 3 mm wide periphery of the wafer.

4.2 Responsivity

Here the measured result of responsivity in consecutive 60-channel WGPD array is described. The 60-channel array is cut off from a 2-inch full-processed wafer, and fabricated by AR coating of $1.3\mu\text{m}$ on the incident facet.

The responsivity was calculated by measuring the photo-

current produced by an incident light with $1.3\mu\text{m}$ wavelength and 0.1 mW power, while an optical fiber is faced to the front facet of WGPD (butt-coupling configuration). A flat-end optical fiber with $6\mu\text{m}\phi$ mode field diameter was used in the measurement. The result is shown in Figure 6. All consecutive 60 channels showed high responsivity of more than 0.95 A/W . The average responsivity was as high as 0.987 A/W , and the standard deviation was 0.011 A/W . Considering the large dimensions of the device -- $250\mu\text{m}$ between elements and 15 mm for the length of 60-channel array-- the variation of responsivity was extremely small. The measurements were carried out with a bias voltage of 5 V , the bias voltage dependence of the responsivity was small at the voltages higher than 1 V .

4.3 Coupling Tolerance

The responsivity (coupling tolerance) in the case of core axis mismatching between the waveguide of WGPD and optical fiber was measured. A single mode fiber of $10\mu\text{m}\phi$ mode field diameter was used. Figure 7 shows the results. Z-axis represents the direction of waveguide, x-axis does

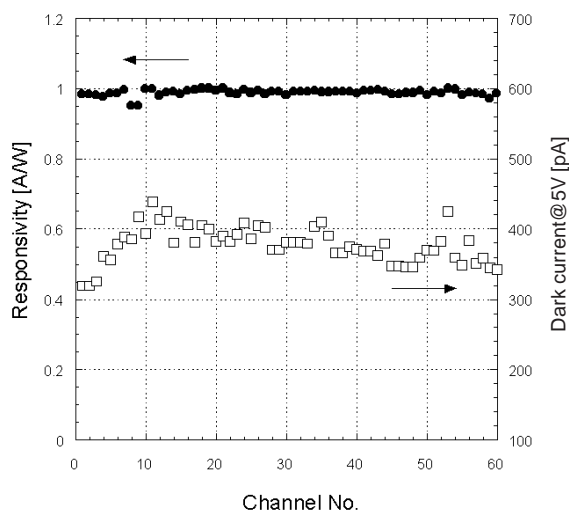


Figure 6 Responsivity in a 60ch WGPD array

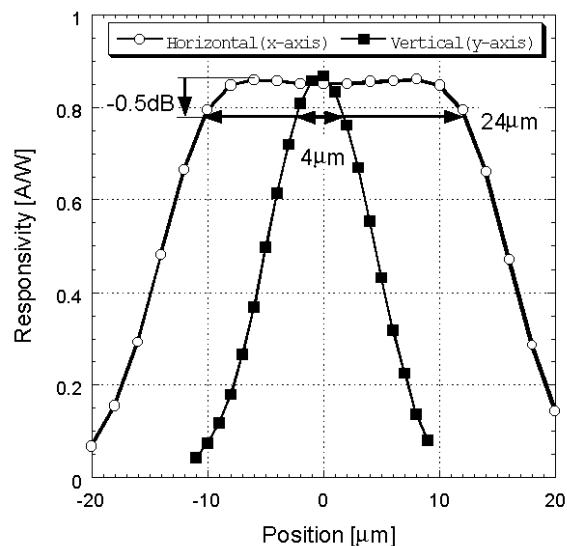


Figure 7 Coupling tolerance in a WGPD

the parallel direction to the wafer and y-axis shows the vertical direction to the wafer. The width of the waveguide of the evaluated device is $30\mu\text{m}$, the tolerance in x-axis direction is $24\mu\text{m}$ in the width in which the responsivity is lowered by 0.5 dB (0.891 times against the peak value). This tolerance is estimated to be wide enough in consideration of the present day surface-mount technology precision. Adopting multi-mode waveguides in y-axis orientation we obtained a good result of $4\mu\text{m}$ in 0.5 dB tolerance degradation.

4.4 Frequency Response

Figure 8 shows the frequency response of waveguide photodiodes evaluating the high-speed characteristics. In order to evaluate the characteristics in array configuration, frequency response characteristics in each channel was measured in 8-ch array. The incident light was $1.3\mu\text{m}$ in wavelength, the intensity was 1 mW . The optical joint of the optical fiber and the device was made by butt-coupling, the same as for the responsivity measurement. In this measurement a standard single mode fiber of $10\mu\text{m}\phi$ in mode field diameter was used. Figure 8 shows that every channel gives the same shape of frequency response which suggests a uniformity good enough in high-speed characteristics. Also Figure 8 indicates that the frequency of lowering by 3 dB in frequency response is approximately 4 GHz . Uneven responses in a certain point in Figure 8 are caused by the noises through the measuring system.

The electrical crosstalk between devices among the 8-ch waveguide photodiodes was measured. The electric signals from an adjacent device to the device, which is jointed to an optical fiber was observed to evaluate the crosstalk components. The electric signals affected by the adjacent device were small enough and less than measurable limits.

4.5 Analog Intermodulation Distortion

The evaluations of intermodulation distortion characteristics of the waveguide photodiode designed and fabricated for analog use are described⁹⁾. Photo 2 shows a prototype

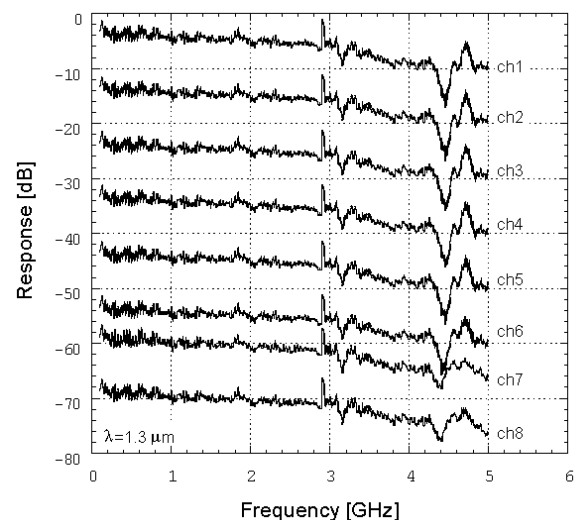


Figure 8 Frequency response in an 8-ch WGPD array



Photo 2 Photograph of analog WGPD pigtail module

of CAN type analog WGPD pigtail module. The measurement of the intermodulation distortion was carried out using 2-tone method. Light signals modulated by different frequencies of 130 MHz and 90 MHz were combined and coupled into the WGPD. The second and third intermodulation distortion components (IMD2, IMD3) among the electrical signal outputs from the photodiode were measured. The optical input power into the photodiode was 1mW. Figure 9 shows the reverse bias voltage dependence of IMD2 and IMD3. When applying enough reverse bias voltages, IMD2 and IMD3 were less than -80 dBc and -100 dBc respectively: both low enough for practical use.

4.6 Reliability

In order to evaluate reliability of the device, an accelerated test was carried out. The accelerated test temperature was 160°C, the reverse bias voltage was 20 V, then dark-currents at room temperature were measured for a given time. Figure 10 shows the results. The increase in dark-current for 5,000 hours was not observed, so the high reliability of the device was confirmed.

5. SUMMARY

The design and fabrication methods for a waveguide photodiode have been studied, which is promising as the long wavelength photodiode for optical subscriber networks. The results of prototypes are reported. We tried a full-process fabrication of 2-inch InP wafer and succeeded in producing devices with high yield and high in-wafer uniformity. The fabricated devices showed a low dark-current, high responsivity, wide coupling tolerance, 4 GHz wide bandwidth, low intermodulation distortion and high reliability.

These WGPDs introduced here are promising candidates for long wavelength photodiodes in optical subscriber networks in the near future, especially for photodiodes in optical integrated circuits.

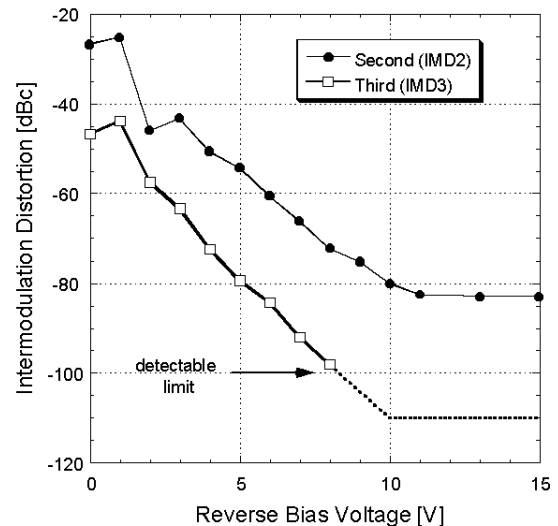


Figure 9 Intermodulation distortion characteristics in an analog WGPD Module

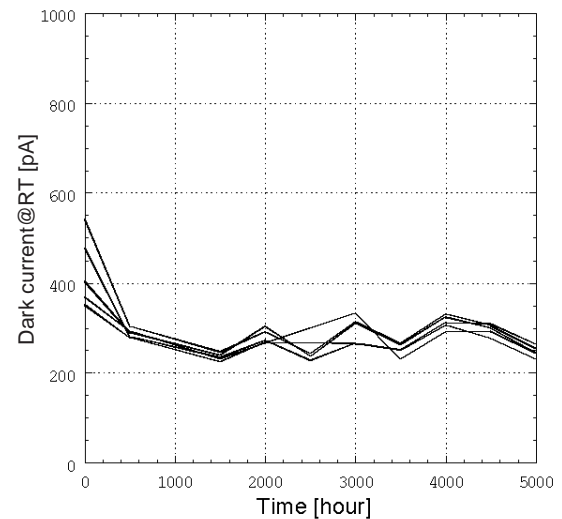


Figure 10 Results of reliability test

REFERENCES

- [1] K. Kato, S. Hata, K. Kawano, J. Yoshida, and Atsuo Kozen: "A high-efficiency 50GHz InGaAs multimode waveguide photodetector", *IEEE J. Quantum Electron.* 28(1992), 2728.
- [2] M. Funabashi, K. Nishikata, K. Hiraiwa, N. Yamanaka, N. Iwai, and A. Kasukawa: "Highly uniform waveguide photodiodes fabricated on a 2-inch wafer with low darkcurrent and high responsivity", *Indium Phosphide and Related Materials (IPRM'98) Proceedings, WA2-3, (1998), p361.*
- [3] K. Nishikata, K. Hiraiwa, M. Funabashi, N. Iwai, N. Yamanaka, T. Wakisaka, A. Kasukawa: "High sensitivity and low intermodulation distortion p-i-n waveguide photodiode modules", *Optical Fiber Communication Conference(OFC'98) Technical Digest, WM10, (1998), 188.*

Manuscript received on October 10, 1998.